31st Congress of the International Council of the Aeronautical Sciences

Belo Horizonte, Brazil; September 09-14, 2018

FATIGUE AND CRACK PROPAGATION LIFE IMPROVEMENT QUANTIFICATION FOR COLD-WORKED HOLES OUTSIDE NOMINAL CONDITIONS

Laura Zaplana*, Ismael Rivero*, Beatriz García-Fogeda*, Javier Gómez-Escalonilla*
***Airbus, Spain**

Keywords: *fatique, fracture, cold-working, XFEM*

Abstract

Cold-working of holes in metal joints is frequently used to improve the fatigue and damage tolerance properties of aeronautical structures. How would its effectiveness change for a hole which conditions have departed from the nominal? This scenario is often found during aircraft structural modifications or major repairs.

In this paper a numerical methodology based on FEM and XFEM simulations to quantify the life enhancement effect of cold-working outside nominal conditions is presented and correlated with test results for a case study scenario.

1 Introduction

One of the main goals of the aerospace industry is to produce larger, lighter, more efficient, less costly and considerably more durable structures. This goal is coupled with the growing need to extend the operational lives of existing aircraft, thus requiring the use of all available means to maximize the fatigue life of the airframe. In this context, holes are of special interest as the highest incidence of aircraft structural fatigue has been associated with holes in fastened joints. One of the methods to extend fatigue life by retarding crack initiation from holes is the generation of permanent compressive stresses via cold working of the fastener holes (as used on bolted or riveted metal joints). This technique is a well-established fatigue life enhancement method which has been used for nearly 50 years [6].

For cold-worked holes in nominal condition, the fatigue life improvements arise from the resultant compressive residual stress field surrounding the plastically expanded hole, leading to a reduction in the mean fatigue stress level in the local regions where cracks eventually initiate. This scenario has been analyzed extensively in the past, and a good understanding and quantification of the fatigue life improvement that this technique provides for aircraft structures can be found in the literature.

In some cases, the cold-worked hole has to be used in conditions that have departed from the nominal. Frequently, going beyond a routine installation is necessary (being a routine installation that one described in the aircraft manufacturer documentation), either because a significant repair is needed or because the use of the cold-worked hole is part of a major structural modification.

In these cases, it is necessary to have the capability of assessing accurately the evolution of the effectiveness of the cold working with the hole diameter (from a fatigue and damage tolerance point of view) in order to determine the limit at which the hole diameter is too large to claim any benefit from the standard cold-working techniques, and this will be the aim of the present study.

In this paper a case study for cold-worked holes at 2024T351 for aircraft wing skin application will be presented. For this case study the effect of the cold-working processes for nominal and non-nominal conditions will be studied. Predictions obtained by analytic models and numerical simulations supported by test evidence will be used to determine the range of validity of cold-working for non-nominal conditions.

2 Cold-working at aeronautical structures

A wide review of the different cold-working technologies that are available for metallic structures can be found in [6], being the most typical application for military transport aircraft at Airbus the "split-sleeve" cold-working. In this technique, a solid tapered mandrel and an internally lubricated stainless steel split sleeve are utilized. The split-sleeve is placed over the mandrel, and the mandrel/sleeve assembly is then inserted into an accurately sized hole. Plastic deformation of the material is generated when the part of the mandrel with a larger diameter moves through the sleeve.

The cold-working process is summarized in the figures below obtained from Airbus internal procedure for cold-working:

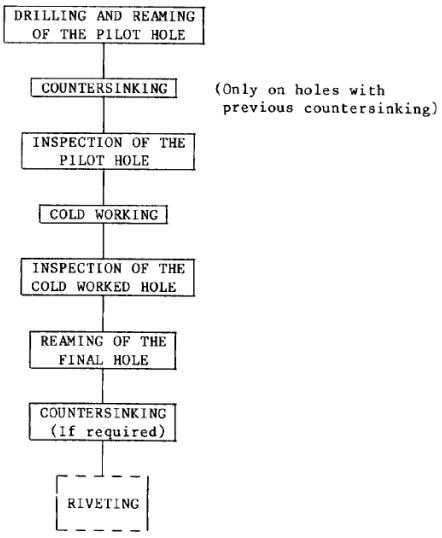

Figure 1: Cold-working process scheme

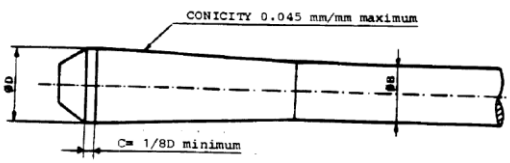

Figure 2: Mandrel used in cold-working process

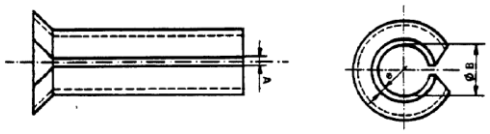

Figure 3: Split-sleeves for cold-working of countersunk holes

Typically two different scenarios for non-nominal configurations can be considered to be representative of the majority of cases:

1) Oversizing of a cold-worked hole without re-applying the cold expansion: the inner layer of the residual compression yield field is removed gradually around the bore up to a certain limit where the residual compressive stress is too low to be considered useful for fatigue protection.

2) Oversizing of a cold-worked hole beyond the maximum diameter allowed in the specification and re-applying the cold expansion afterwards.

3 Methodology for cold-working effect evaluation

In this chapter the different methodologies that will be used to evaluate the effect of the cold-working for the case study presented in this paper will be explained. The evaluation will be focused on two topics:

1) Residual stress field after cold-working process

2) Effect of cold-working residual stress field over crack propagation life

3.1 Calculation of cold-working residual stress field

3.1.1 Analytic evaluation

The prediction of residual stress fields for cold-worked holes is a key factor to determine the final effect that the cold-working process will produce over the fatigue and crack propagation life of aeronautical structures.

In the literature many analytic formulations for this purpose can be found. An evaluation of the accuracy of several of these analytic models for different material applications was performed found in [7]. For 2024T351 Ball model defined in [8] provided the best correlation with test results. Therefore for the studies included in this paper, this analytic method will be considered. The material

parameters corresponding to 2024T351 for Ball model application are also provided in [7].

3.1.2 Cold-working simulation

The cold-working process is simulated using a finite element model analysed with Abaqus 2017. An implicit simulation is performed obtaining the stress field due to the hole expansion during the cold-working and the final residual stress field at the end of the process.

The cold-working is simulated through the pressure applied at the hole surface by the mandrel during the process due to the interference between the mandrel with the sleeve and the hole.

The material plastic response and hardening behaviour has a very relevant influence over the obtained results, as discussed in [7]. The modelization of material properties has been calibrated and validated by correlating a 2D finite element model in plane stress conditions with the analytic results predicted by Ball model. Once calibrated, material properties can be applied to the specific case study simulation to obtain the corresponding residual stress conditions.

3.2 Evaluation of cold-working effect over crack propagation life

Conventional Finite Element Methods are often not practical and efficient for Fracture Mechanics due to the needed flexibility to follow crack propagation without the use of fine meshed models. Also, re-meshing is necessary, what leads to an important processing time and cost. Therefore, advanced numerical methods appear here as the most adequate procedure to solve these kind of problems. Many methods have been developed. Among them, it can be found the group of meshless methods [1] that combine the flexibility due to the non-dependency on the elements with the more or less ease to redistribute the control points to solve the algorithms.

In this paper, authors have chosen eXtended Finite Element Method (XFEM, [2] and [3]) to analyze the crack propagation at cold-worked scenarios. The selection of this methodology is sustained in the fact that XFEM is using a preexisting FE mesh, what makes it a great candidate to be used in the industry because it is easy to move from FEMs (normally used by the engineers in the conventional analysis) to XFEM.

3.2.1 eXtended Finite Element Method

In this chapter, the basic concepts of the XFEM are introduced. Further and more extensive information about this meshless method (MM) can be found in [2] and [3].

As stated in the previous paragraph, XFEM is included in the group of numerical methods for solving Parcial Derivative Equations (PDEs) called Meshless Methods (MMs). These methods are developed in order to solve the PDEs avoiding the use of meshes, completely or partially.

Within this group of MMs, XFEM is based on the enrichment of solution-type functions by adding new degrees of freedom to the predefined traditional FEM mesh. These additional degrees of freedom are arbitrarily located depending on the problem to be solved.

This is the main advantage of this numerical method for the cases studied in this paper for crack growth: the flexibility and adaptability to the geometry of the domain under investigation.

In [2] and [3], the main general formulation of the equations representing XFEM solutions are introduced. The equation representing the typical case studied within this paper (crack growth, considering the crack as a discontinuity) is shown next:

$$\mathbf{u}^h(\mathbf{x}) = I + J + K \qquad (1)$$

where:

$$I = \sum_{i \epsilon I} \phi_i(\mathbf{x})\, \mathbf{u}_i \qquad (2)$$

Being u_i the nodal parameters of the entire set of nodes (Set I) and $\phi(x)$ the corresponding shape functions.

$$J = \sum_{j \epsilon J} \phi_j(\mathbf{x})\, \mathbf{b}_j H(\mathbf{x}) \qquad (3)$$

Being b_j the nodal enriched degrees of freedom for the nodes of the elements that are fully cut by the discontinuity (Set J), and H(x) the jump-function.

$$K = \sum_{k \epsilon K} \phi_k(\mathbf{x}) \left(\sum_{l=1}^{4} \mathbf{c}_k^l F_l(\mathbf{x}) \right) \qquad (4)$$

Being $c_{k,l}$ the nodal enriched degrees of freedom of the nodes of the element where the crack tip is located, and $F_l(x)$ adequate asymptotic functions for the displacement field near the discontinuity tip (Set K).

3.2.2 Introduction to iCracx

In [4] a detailed evaluation and validation of Abaqus XFEM capabilities was performed. As a consequence of this evaluation, it was concluded that Abaqus offers a robust XFEM methodology to perform SIF and J-integral calculations; however some major limitations affect the crack propagation simulations related mainly to compatible material models, introduction of contacts and complex loading applications. These limitations usually have an impact over the efficiency of Abaqus to perform Crack Propagation simulations for actual industrial cases. To overcome these limitations, Airbus, with the collaboration of Safran Engineering Services, launched the development of a Python software tool, named iCracx (improved Crack Abaqus computation with XFEM), capable to perform crack propagation simulations without a pre-defined crack path (solution-based propagation) calculating simultaneously Stress Intensity Factor and J-integral calculations without the limitations in terms of contacts, material model, loading spectra complexity, etc., inherent to the approach implemented in Abaqus.

Next figure shows the basic scheme of iCracx.

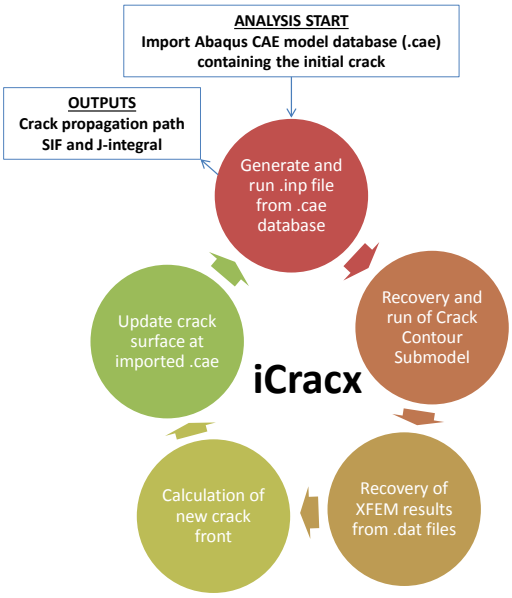

Figure 4: iCracx basic workflow

Initial version of iCracx (iCracx v1), used in [4], was able to perform a full crack propagation simulation considering only a single crack. A set of validation cases was included to ensure iCracx robustness and accuracy.

Due to the necessity of providing iCracx with multicrack capabilitites, a new version (iCracx v2) has been developed by Airbus. This new version is able to perform a full crack propagation simulation allowing an arbitray number of cracks growing simultaneously and interacting each other. The same philosophy and capabilities of initial iCracx version are maintained. iCracx has been developed to run Abaqus 6.14-2 and later. This version was validated by Airbus in [5].

4 Wing lower skin case study

The effect of hole cold-working is assessed for a 2024T351 alloy case under 3 different conditions of split-sleeve cold working:

Type I) no cold working

Type II) nominal cold working (hole diameter within the limits of the cold working specification norm)

Type III) non-nominal cold-working (hole diameter outside the limits of the cold-working specification norm).

This case study is performed for the configuration shown in next figure. The cold-working is applied at the 3 fastener holes. The configuration is based on an actual application for transport aircraft wing lower skin attachment to reinforcement doubler.

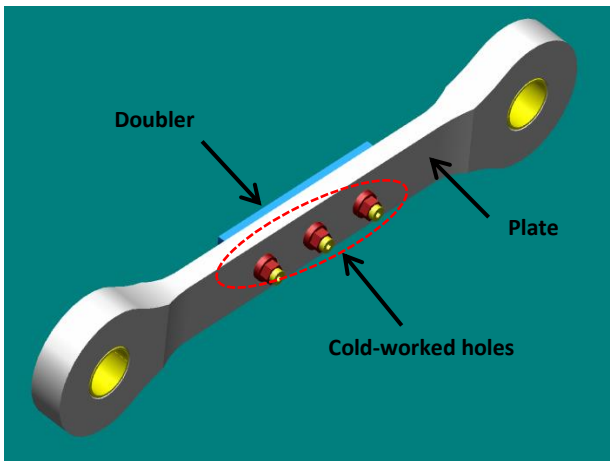

Figure 5: Studied configuration

The effect of the 3 conditions over the fatigue and crack growth lives will be assessed under a typical wing lower skin loading spectrum. The applied loading spectrum contains 3300 different simulated flights.

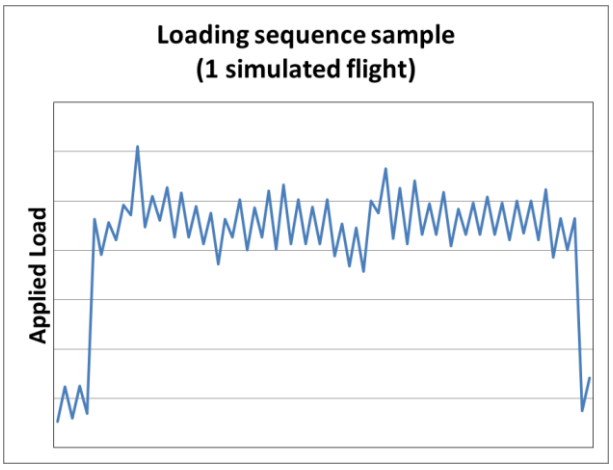

Figure 6: Case study sample loading sequence

4.1 Test Results

Fatigue tests were conducted for three different set of coupons of 2024T351 (Type I, Type II and Type III conditions).

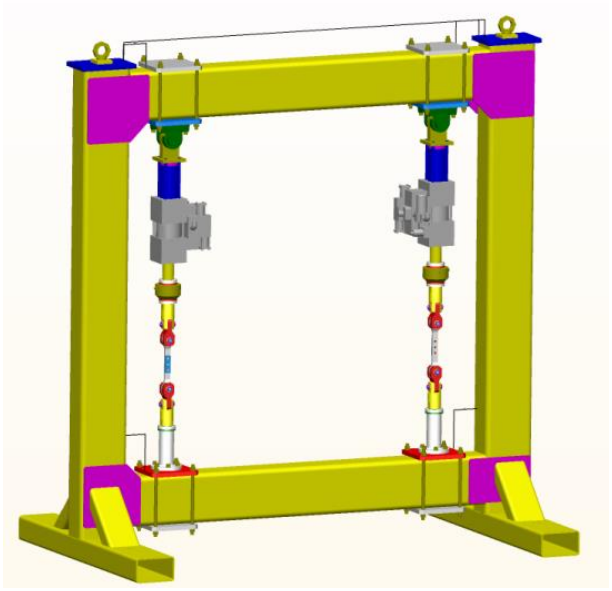

Figure 7: Test rig

The obtained test results are shown in Figure 8 below, where the equivalent stress cycles to failure are represented. The first set of coupons in blue corresponds to Type I, the second set in red to Type II and the third set in yellow to Type III coupons.

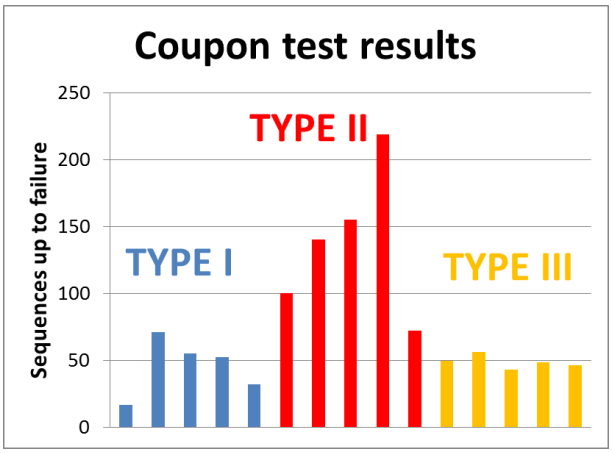

Figure 8: Test Results – Equivalent stress cycles to failure

As can be seen from Figure 8, Type II coupons have appreciably more fatigue life than the other two types but with higher dispersion. The Type III coupons have a similar fatigue life than Type I coupons.

From the test results, a fatigue life improvement factor of 1.057 was determined for Type III coupons with respect to Type I coupons. Therefore, it can be concluded that the non-nominal coldworking is not effective, as the

fatigue lives are virtually the same as for those specimens without coldworking. A fatigue life improvement factor of 2.77 was determined for Type II with respect to Type I coupons, which represents the life improvement introduced by cold working in nominal conditions.

4.2 Numerical Simulation Results

In this chapter the results for the numerical simulations performed for Type I, Type II and Type III configurations are included. The scheme for the calculation process is shown in the next figure:

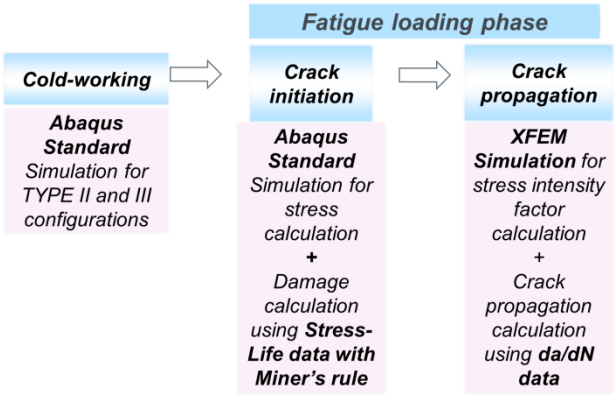

Figure 9: Calculation approach

The finite element model used as baseline for the simulations is shown in the next figure.

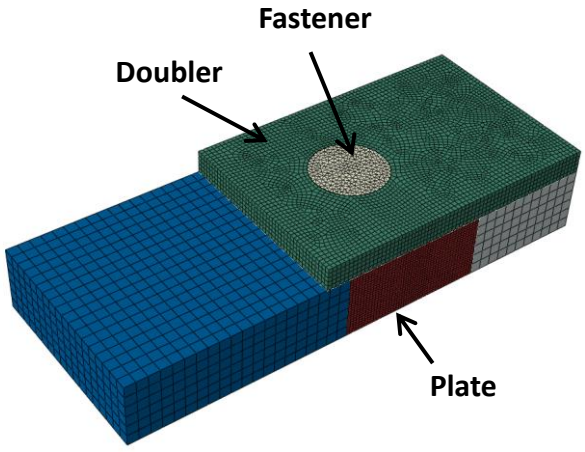

Figure 10: Case-study finite element model

4.2.1 Cold-working simulation

In the next figure the analytic predictions for Type II and Type III configurations are shown.

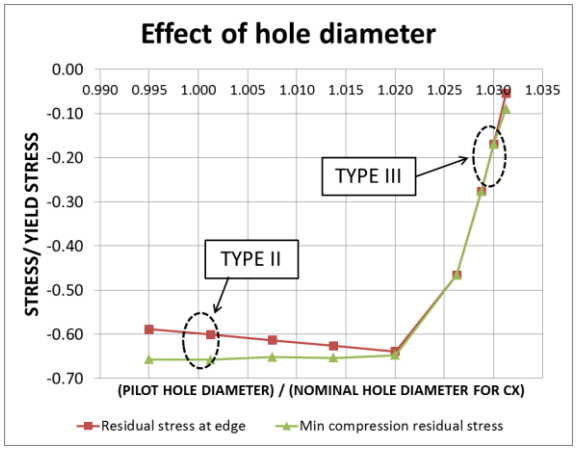

Figure 11: Cold-working analytic stress fields

The material behaviour modelling for the cold-working simulation is validated through the comparison of the analytic results for Type II configuration (nominal cold-working) with a 2D plane stress finite element model. This model is used as it represents the conditions for which Ball analytic model was developed. By validating material behaviour for this condition, the modelization of this behaviour can be then applied to the finite element model developed for the case study. In addition the comparison between the residual stress field results for plane stress and plane strain finite element model is included to quantify the effect of this condition over the cold-working, as the proposed case-study shows plane strain behaviour due to the high thickness of the plate (≈12mm). The obtained results in this calibration and validation process are shown below:

Residual stresses after cold-working / Yield stress		
Calculation	**At hole edge**	**Min compression**
Ball method	-0.60	-0.66
Plane Stress FEM	-0.59	-0.65
Plane Strain FEM	-0.70	-0.81

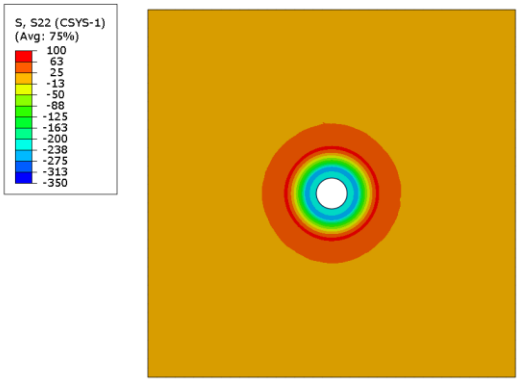

Figure 12: Plane stress residual stress field

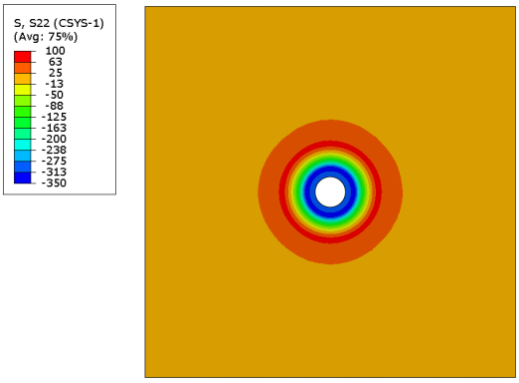

Figure 13: Plane strain residual stress field

The cold-working stress fields for Type II and Type III cold-working configurations* obtained through the numerical simulation with the material modelling validated through the correlation of the 2D model are shown in the next figures.

**For Type I configuration, no cold-working is applied*

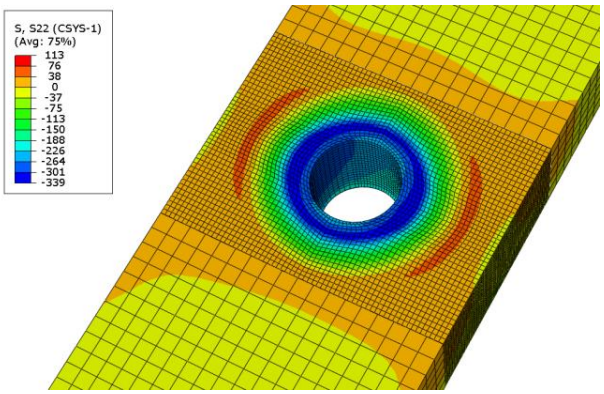

Figure 14: Cold-working numerical simulation – Type II

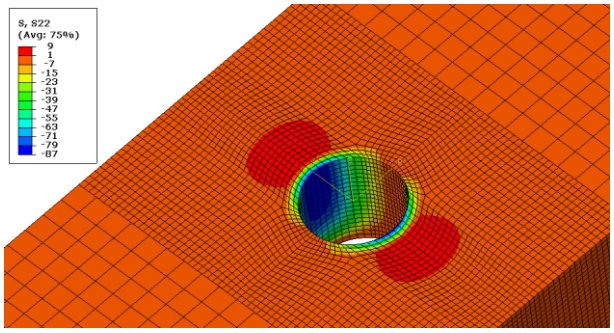

Figure 15: Cold-working numerical simulation – Type III

4.2.2 Fatigue life calculation

For fatigue life calculation, the finite element model is used to obtain the relation between the applied load at the plate and the notch stress at the hole edge. This relation will be applied to the loading sequence to obtain the equivalent notch stress sequence that will be used to calculate the corresponding fatigue life based on 2024T351 Stress-Life (SN curve) data.

In the next figures the stress fields at the plate hole for an applied gross stress of 200MPa are shown for Type I, Type II and Type III configurations.

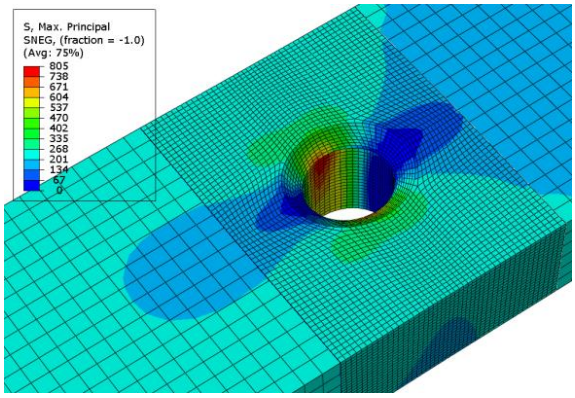

Figure 16: Stress plot Type I configuration

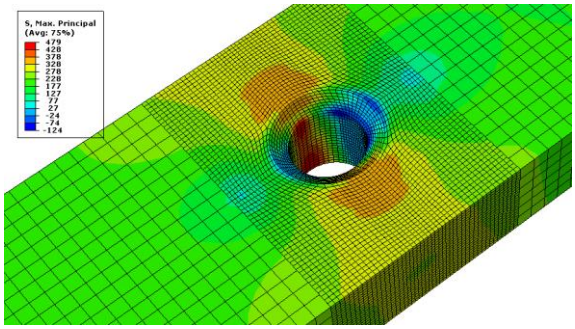

Figure 17: Stress plot Type II configuration

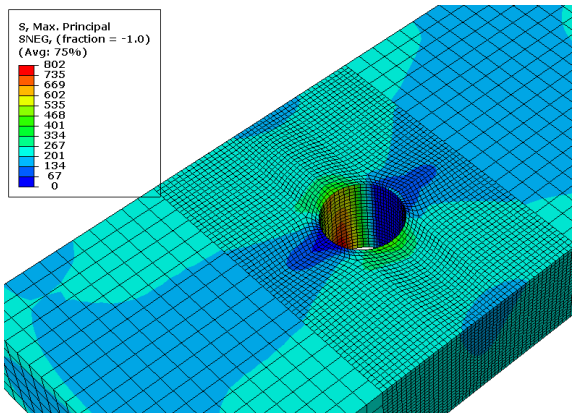

Figure 18: Stress plot Type III configuration

The calculated fatigue lives for the 3 configurations are shown in the next table compared with the average test failure among all the tested coupons for each configuration.

Config.	Number of applied load sequences up to failure	
	Calculated	Test average
TYPE I	32.62	46.14
TYPE II	122.74	137.29
TYPE III	33.25	48.81

The Life Enhancement Factors (LEF) for the nominal (Type II) and non-nominal (Type III) cold-working processes are included in next table:

Config.	Life Enhancement Factors	
	Calculated	Test average
TYPE II	3.76	2.98
TYPE III	1.02	1.05

An acceptable correlation with test results is obtained in the LEFs calculations taking into account the dispersion in test results obtained for Type II cold-working.

4.2.3 Crack growth life calculation

For crack growth calculation, a scenario with an initial crack of 1.27mm growing from the location at the hole edge with the highest notch stress is considered. This scenario was observed in test coupons as shown in the figure below.

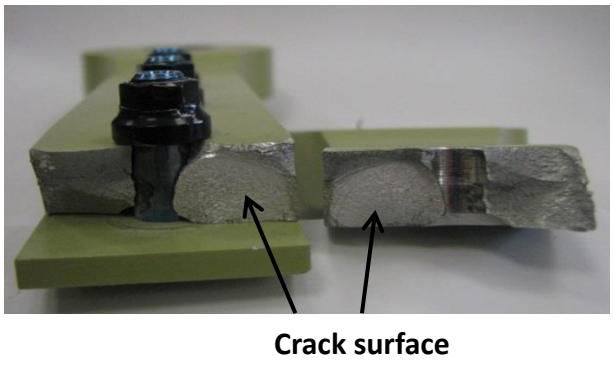

Figure 19: Crack at test coupon

The evolution of the stress intensity factors as a function of crack length is obtained using Airbus iCracx software based on Abaqus XFEM methodology as explained in chapter 3. In the next figure, the crack evolution at an intermediate growth step is shown as sample.

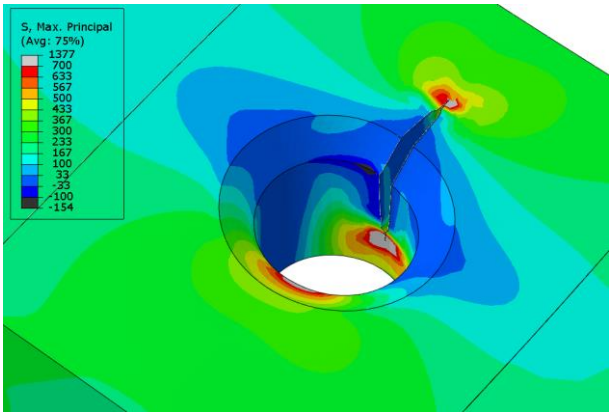

Figure 20: Crack growth simulation

A sensitivity study has been performed to determine the enrichment radius for J-integral / Stress Intensity Factor (SIF) calculation at crack tip providing the better results convergence.

SIF results are provided in terms of Normalized SIF as defined in the equation below where σ is the applied gross stress and a is the crack length.

$$Norm.SIF = \frac{SIF}{\sigma\sqrt{\pi a}} \qquad (5)$$

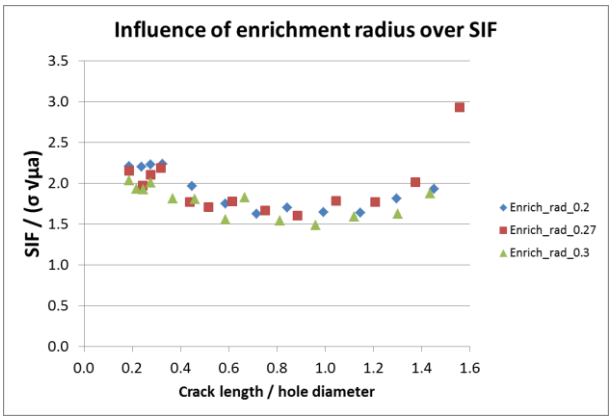

Figure 21: Influence of enrichment radius over Stress Intensity Factor

The SIF calculation with iCracx has been performed for the 3 configurations (Type I, Type II and Type III) and the obtained results are shown in next figures for crack front at through-width direction (Tip A) and through-thickness direction (Tip B).

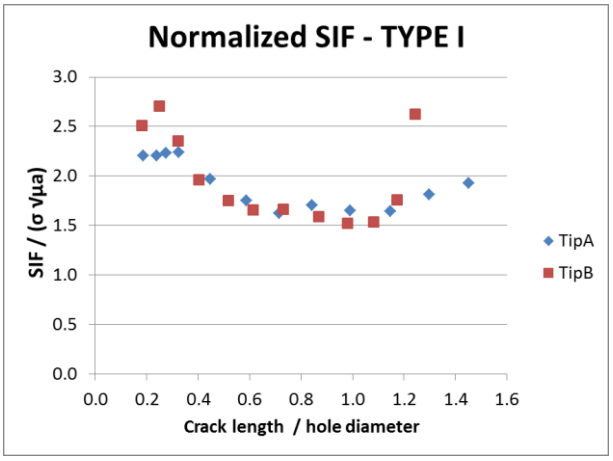

Figure 22: SIF results – Type I configuration

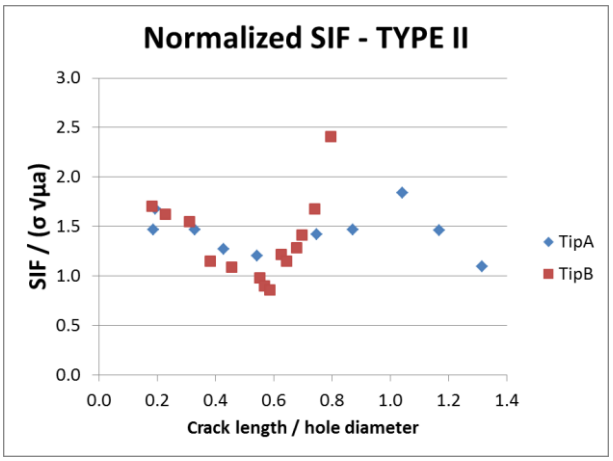

Figure 23: SIF results – Type II configuration

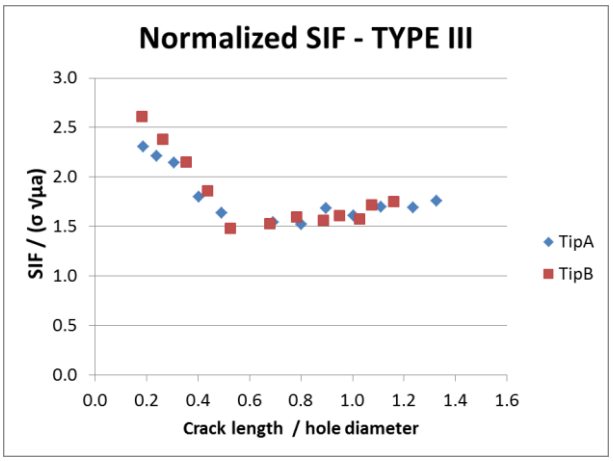

Figure 24: SIF results – Type III configuration

Comparing the crack surfaces obtained with the iCracx simulations with fracture surfaces at test coupons it can be observed that an equivalent behaviour is obtained for cold-worked and no cold-worked coupons.

- Type I and III: crack becomes through-part before reaching the lateral edge

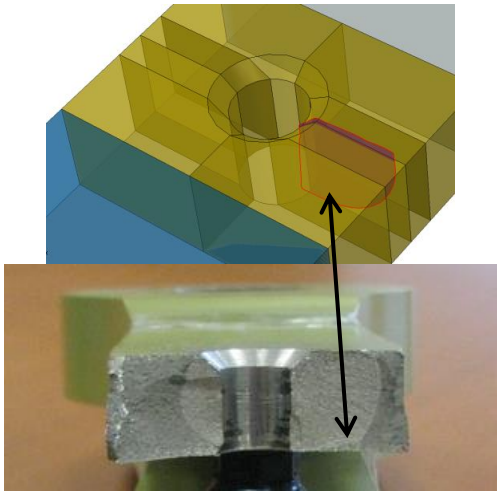

Figure 25: Crack surface – type I and III

- Type II: crack reaches the lateral edge of the coupon before becoming through-part

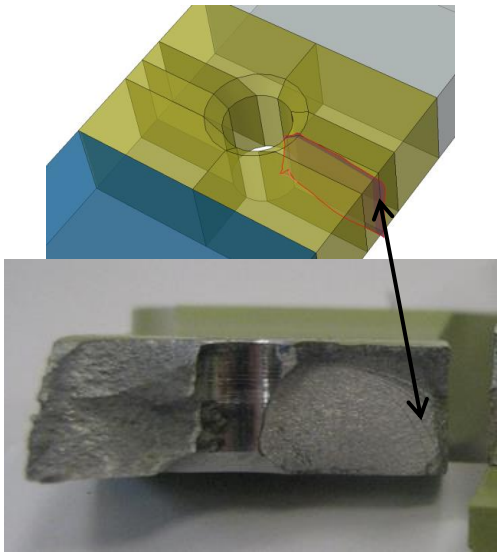

Figure 26: Crack surface – type II

Knowing the evolution of the Stress Intensity Factors in function of the crack length, a crack growth analysis from typical manufacturing flaw size considered in aircraft damage tolerance analysis to final failure has been performed using 2024T351 da/dN data.

The calculated crack growth lives for the 3 configurations are shown in the next table.

Config.	Life from initial crack to failure (flights)
TYPE I	2079
TYPE II	12823
TYPE III	2576

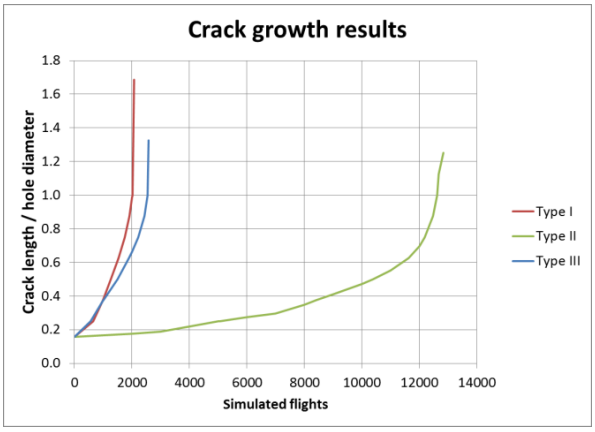

Figure 27: Crack propagation comparison

From the previous figure it can be seen that Type II cold-working is leading to a significant increment in the crack growth live. However the percentage of crack propagation phase over total life is lower than 10% for the 3 configurations therefore the influence over life enhancement factor of crack growth phase is limited for this case study.

5 Conclusions and way forward

In this paper a methodology for the evaluation of the effect of cold-working at fastener holes for nominal and non-nominal conditions over fatigue and crack growth behaviour has been presented. This evaluation has been performed through numerical simulations based on the conventional finite element method (FEM) and the extended finite element method (XFEM) supported by analytic validation and test correlation.

Future studies will be focused on the correlation of the crack propagation phase, both Stress Intensity Factors and crack path, with test measurements as available test experience was focused on fatigue failure. Future investigations will also include the evaluation of the effect of cold-working for Widespread Fatigue Damage scenarios.

Contact Author Email Address

The authors can be contacted in the following email address:
laura.zaplana-manzano@airbus.com

Acknowledgments

The authors want to recognize the support provided by their colleagues at Airbus during the development of this work, especially for their colleagues at Military Aircraft Fatigue and Damage Tolerance Team and Stress Methods Team. Without their support it would have not been possible to reach the proposed goals within this project.

References

[1] Fries, T.; Matthies, H. (2004). Classification and Overview of Meshfree Methods. Institute of Scientific Computing, Technical University Braunschweig, Brunswick, Germany.

[2] Belytschko, T.; Black, T. (1999). Elastic crack growth in finite elements with minimal remeshing: Int. J. Numer. Methods Eng., 45(5), 601– 620.

[3] Moës, N.; Dolbow, J.; Belytschko, T. (1999). A finite element method for crack growth without remeshing: Int. J. Numer. Methods Eng., 46, 131–150.

[4] Rivero, I.; Gómez-Escalonilla, J. XFEM-based fracture mechanics analysis of aeronautical structures affected by residual stresses: 30th Congress of the International Council of the Aeronautical Sciences, DCC, Daejeon, Korea, September 25th – 30th 2016.

[5] Rivero, I.; Valencia, O.; Martin, N.; de Nicolas, B.; Gómez-Escalonilla, J. Improving MultiSite Damage (MSD) Fracture Mechanics Analysis using XFEM. NAFEMS World Congress 2017, Stockholm, Sweeden, June 11th – 14th 2017.

[6] Yucan, F.; Ende, G.; Honghua, S.; Jiuhua, X.; Renzheng, L. (2015) Cold expansion technology of connection holes in aircraft structures: A review and prospect. Chinese Journal of Aeronautics, 28(4), 961-973

[7] Wang, Z.; Zhang, X. (2003). Predicting fatigue crack growth life for cold-worked holes based on existing closed-form residual stress models. International Journal, 25, 1285-1291.

[8] Ball DL. (1995). Elastic-plastic stress analysis of cold expanded fastener holes. Fatigue Fract Eng Mater Struct; 18:47-63

Copyright Statement